Regular Article

ANALYTICAL AND BIOANALYTICAL CHEMISTRY RESEARCH

Published by the Iranian Chemical Society

Anal. Bioanal. Chem. Res., Vol. 8, No. 4, 453-466, September 2021.

Construction of Electrochemical Sensor Modified with Molecularly Imprinted Polymer and rGO-Fe_3O_4-ZnO Nanocomposite for Determination of Bisphenol A in Polymers and Water Samples

Hamid Reza Movahed[a], Mosayeb Rezaei[b,*] and Zahra Mohagheghzadeh[b]

[a]*Department of Technical and Engineering, Islamic Azad University Yadegar-e-Imam Khomeini (RAH) Shahr-e-Rey Branch, Tehran, Iran*

[b]*Knowledge-based Department, Farapol Jam Chemical Industrial, Hamedan, Iran*

(Received 31 December 2020 Accepted 31 May 2021)

A modified molecularly imprinted polymer-carbon paste electrode (CPE) with rGO-Fe_3O_4-ZnO nanocomposite was constructed and used for the determination of Bisphenol A (BPA) using differential pulse voltammetry (DPV) technique. The rGO-Fe_3O_4-ZnOMIP/CPE shows a sharp and well-defined peak for the oxidation of BPA at 648 mV in Britton-Robinson universal buffer solution pH = 6.5. The presented electrode shows a dynamic range of 0.008-15 and 15-95 µM with a low detection limit of 0.004 µM. The repeatability, reproducibility, and stability of rGO-Fe_3O_4-ZnOMIP/CPE were checked and the obtained data confirm the excellent properties of the sensor. The selectivity of the presented method was investigated and the data show that Hydroquinone, Tert-butyl hydroquinone, Catechol and Bisphenol S and common ions had no disturbance on the detection of BPA and the changing in peak current was below 5%. Finally, rGO-Fe_3O_4-ZnOMIP/CPE was successfully applied for the determination of BPA tap water, food storage container and cured vinyl ester resin samples with satisfactory results.

Keywords: Bisphenol A, Molecularly imprinted polymer, Carbon paste electrode, rGO-Fe_3O_4-ZnO, Electrochemical determination

INTRODUCTION

2,2-Bis(4-hydroxyphenyl) propane or Bisphenol A (BPA) is used as one of the main raw materials in the synthesis of some polymers such as epoxy resin and vinyl ester resin, and other product such as polycarbonate [1]. Also, BPA has been used in the produce of metal can coatings, different type of water baby bottles and baby food storage containers, polycarbonate beverage bottles and dental fillings [2]. Trace amounts of the packaging materials could migrate into water and food, which can be eaten with them. BPA is one of the Endocrine-disrupting compounds which can produce undesirable effects on the systems of human hormones. BPA could affect the reproductive system; it could affect the result in neural and behavioral changes in infants and children reproductive [3,4]. Also, BPA can cause some cancers, including breast, prostate, and testicular cancer. Besides, other diseases caused by BPA exposure include diabetes, cardiovascular diseases, hyperactivity and obesity. Nowadays, the United States and the European Union countries put BPA on the blacklist of pollutants [4]. Therefore, it is essential to develop a simple, rapid, and sensitive determination method of BPA in order to administrate the environmental BPA pollution. Several techniques have been reported for the determination of BPA that some of them are mentioned below.

Chromatographic Methods

Zhang *et al.* used solid-phase extraction-high performance liquid chromatography (SPE-HPLC) for the determination of BPA in an aqueous solution [5]. Zhuang *et al.* design a new method by the combination of a new spectrophotometric method and HPLC for the measurement of BPA at 410 nm in hot water [6]. Zou *et al.* prepared a

*Corresponding author. E-mail: mosayebrezaei@gmail.com

BPA imprinted monolithic pre-column to online solid-phase extraction for HPLC. They determined successfully phenolic compounds in river water [7]. Haginaka *et al.* develop a new method by the combination of isotope imprinting and LC-mass spectrometry for the determination of BPA and its halogenated derivatives in river water [8]. Park *et al.* extract BPA directly and determine it by gas chromatographic-mass spectrometric method [9].

Spectrophotometric Method

Xu *et al*. applied a sensitive spectrophotometric method using a diazotization-coupling reaction to the measurement of BPA. The parameters which can affect the signal such as reagent concentration and pH were optimized. The obtained data were compared with HPLC, and the presented method was applied to the determination of BPA in real samples include milk and water bottle samples [10]. Sun *et al.* present a new method base on fluorescence spectrophotometry to direct measurement of BPA in aqueous solution and pH = 8 at λ_{ex} = 266 and λ_{em} = 304 nm [11]. Kum *et al.* developed a rapid spectrophotometric detection method for BPA in environments base on the blue color formation of the BPA/ferric chloride/ferrocyanide complex [12].

Although chromatographic methods are commonly used for the determination of some molecules like BPA, some features such as time-consuming analysis, costly instrumentations, complex sample pretreatment process and dependence on the operator for spiking of the sample, led to developing new methods for measuring this molecule [13]. In recent decades, sensor-based methods have been developed for the determination of molecules and ions. Among these methods, the electrochemical sensors have better advantages such as low-cost instruments, easy operation, reliable data, high accuracy, fast response, simple real sample pretreatment [14-17]. So, in this research, the new electrochemical sensor was designed for the determination of the analyte.

Nonspecific-binding, low selectivity and poor regeneration are the problems of direct measurement electrochemical methods [18]. There are some methods and materials to overcome these disadvantages. Molecularly imprinted polymers (MIPs) are one of the best artificial materials for preparing chemical sensors methods in order to increase the selectivity and specific-binding [19]. The high physical/chemical and mechanical stability such as high pressure, high temperature, stability versus acid/base or organic solvents, low-cost preparation, supreme binding affinity, and economic production are the specific properties of MIPs [19,20]. The electrochemical sensor base on MIPs can determine a wide variety of materials include food additives, metals ions, microbial cells, and drugs [21-26].

Nowadays, some nanomaterials such as carbon base NPs (*e.g*. graphene) and metal oxide NPs (*e.g*. ZnO and Fe_3O_4) are used as a catalyst for improving the sensor performance [27,28]. ZnO NPs as an environmentally friendly semiconductor (band-gap ~ 3.37 eV) has been applied in electrochemical devices because of their non-toxicity, proper sensing behavior, physical and chemical stability [29]. Fe_3O_4 NPs as a superparamagnetic material, due to biocompatibility, low toxicity, catalytic activity, large surface areas, and simple preparation commonly used in different industries and especially in sensing applications in order to provide a maximum signal [30]. Graphene nanosheet (Gr) as a zero band-gap semiconductor has unique properties include large surface area, and high electrical conductivity because of abundant electrochemically desirable edge carbons per mass of Gr which comfort electron transfer between analytes and the surface of the sensor by a low over-potential [31]. So, they are good candidates for use in electrochemistry. In recent years, metal oxide loading or doping on Gr was used to promote the catalytic property of NPs due to the synergetic effect between NPs into nanocomposites [32].

These unique properties have opened a new window of possibilities for developing new analytical methods. In this way, an innovative way to synthesize novel MIPs is the incorporation of nanoparticles into their structure. The combination of these two materials (polymer and nanoparticles/nanocomposites) gives rise to a hybrid material with potential and new properties. In general, MIPs are classified into two types according to whether they are obtained as a single continuous and porous piece (molecularly-imprinted monoliths, MIMs) or as individual nano/microparticles (MIP micro/nanoparticles). Some nanoparticles, such as metal oxide, carbon nanoparticles, or molecular sieves, can be acted as main monomers or scaffolds of the monolithic structure. In contrast, in the

synthesis of MIP nanoparticles, the role of nanoparticles, generally, is to act as the core or support of the imprinted polymer film. On the other hand, nanoparticles can increase the surface of the sensor and also the electrochemical site of reaction, so the use of nanoparticles can improve the signal-to-noise ratio, the performance of the sensor, and sensitivity and detection limit of the presented electrode to the determination of BPA.

In this study, the use of the rGO-Fe_3O_4-ZnO@MIP as a sensing layer, which was mixed with the carbon paste matrix for the voltammetric determination of BPA in spiked and real samples is described. Good conductivity and selectivity of the proposed sensor on BPA were well observed which lead to obtaining a wide linear range (LR) with a low detection limit (DL).

EXPERIMENTAL

Chemicals

BPA, methacrylic acid, GO, ferrous chloride tetrahydrate, ferric chloride hexahydrate, sodium hydroxide, oleic acid, ethylene glycol dimethacrylate, polyvinylpyrrolidone, azobisisobutyronitrile, zinc acetate dihydrate, graphite, paraffin oil, sodium borohydride, were provided from Sigma-Aldrich and Merck Company (Darmstadt, Germany). All the solutions and materials used were of analytical grade. Deionized distilled water (DDW) was used for the preparation of solutions. The Britton-Robinson buffer solution (B-R) applied to adjust the pH value and as a supporting electrolyte.

Apparatus

Electrochemical experiments were performed at ambient temperature (about 25 °C) using a Behpajoh potentiostat/galvanostat system (model BHP-2065, Iran). The electrochemical cell was congregated with a conventional three-electrode system by an Ag/AgCl (Azar electrode, Iran), platinum wire and unmodified/modified carbon paste electrodes (CPE) as the reference electrode, auxiliary electrode and working electrodes, respectively. The pH value measurements were done by a Metrohm pH meter (model 713, Herisau, Switzerland). The structure and morphology of the synthesized nanomaterials were investigated by scanning electron microscope (SEM) SEM-EDX, Philips, XL30 (Netherland), X-ray powder diffraction (XRD) 38066 Riva, d/G. *Via* M. Misone, 11/D (TN) Italy and Fourier transform infrared (FTIR) Perkin Elmer, spectrum 100 (USA).

Preparation of the Materials

Fe_3O_4 NPs. The coprecipitation method was used for the synthesis of Fe_3O_4NPs. In the first step, 0.01 and 0.02 mol ferrous chloride tetrahydrate and ferric chloride hexahydrate, respectively, were added to 100 ml DDW in a 250 ml three-necked flask. The N_2 was purged while the solution was stirred continuously, and the temperature was increased to 80 °C. In the next step, sodium hydroxide solution (40 ml, 2 M) was added to the heated solution and mixed for 1 h. The synthesized magnetic precipitates were collected by the external magnetic field when the solution temperature reached about 25 °C. Finally, the obtained Fe_3O_4 NPs were washed by DDW five times and dried at 70 °C in the oven.

ZnO NPs. In order to synthesis ZnO NPs, 1 g zinc acetate dihydrate was added to 250 ml three-necked flask containing 100 ml ethanol solution. The mixture was stirred for 20 min then 0.25 M of sodium hydroxide in ethanol was added slowly until the pH reached 8.0. The mixture was stirred for 4 h then filtered and washed by DDW five times and dried at 70 °C in the oven.

Reduced graphene oxide (rGO). The rGO was synthesis by the addition of sodium borohydride as a chemical reduction reagent to purchased GO. Firstly, 150 mg purchased GO was dispersed into 150 ml DDW and sonicated for 20 min after that 2 ml sodium borohydride was added to the mixture and the temperature increased to 100 °C and kept for 10 h. The obtained rGO was centrifuged, washed by DDW five times and dried at 80 °C in the oven.

rGO-Fe_3O_4 nanocomposite. For this goal, 0.1 g synthesized rGO was added to 50 ml of DDW:ethanol (1:1 V/V) and sonicated for 25 min to obtain the uniform suspension. After that 0.4 g Fe_3O_4 NPs was added to the suspension and mixed for 1 h. The temperature of the solution was increased to 105 °C and kept for 24 h in order to do a hydrothermal reaction. The obtained participate was filtered and washed by DDW five times and dried at 70 °C in the oven.

rGO-Fe_3O_4-ZnO nanocomposite. The target nanocomposite was synthesized by the same method as the rGO-Fe_3O_4 nanocomposite, only 0.2 g Fe_3O_4 NPs and 0.2 ZnO NPs were added to rGO suspension[33].

Preparation of MIP, Modified MIP and NIP

The modified MIP was synthesized as follows: the 1.2 mmol BPA was dissolved in 10 ml water:methanol (8.5:1.5, v/v) and 8.0 mmol methacrylic acid were stirred for 45 min for the preparation of the solution (I). Then 0.6 g of each NPs or nanocomposites were mixed with 1.0 ml oleic acid and stirred for 15 min to prepare a solution (II). Then, 20 mmol ethylene glycol dimethacrylate and the solution (I) were added to the solution (II). This mixture was subjected to ultrasound for 40 min for the preparation of the pre-polymerization solution. After that, 0.4 g polyvinylpyrrolidone was dissolved in 100 ml ethanol in a three-necked round-bottomed flask. The mixture was stirred at 300 rpm and purged with N_2 gas while the temperature increased to 60 °C. The pre-polymerization solution was added into the three-necked flask, then 0.1 g azobisisobutyronitrile was also added to it. The reaction was allowed to proceed at 60 °C for 24 h. After the polymerization, the polymers were separated by the external magnetic and washed with methanol:acetic acid (8:2, v/v) several times, then washed with methanol several times. Then, the polymers were rewashed with water three times and dried at 60 °C. Also, the NIP was prepared with processing similarly as above, except that the template molecule BPA was not added.

Construction of Modified CPEs

The unmodified CPE was constructed by completely hand mixing the 75 w/w% graphite powder with the 25 w/w% paraffin oil in a mortar using a pestle. An appropriate amount of the obtained mixture was packed stoutly into an insulin syringe as an electrode body (Internal diameter:height is 2.5:300 mm). The packing process was carefully done to avoid possible air gaps because leading to an increase in the electrical resistance of the electrode. In order to establish electrical contact, a clean copper wire was put into the end of the packed electrode. The modified electrodes include MIP/CPE, NIP/CPE, GOMIP/CPE, rGOMIP/CPE, Fe_3O_4MIP/CPE, ZnOMIP/CPE, rGO-Fe_3O_4MIP/CPE and rGO-Fe_3O_4-ZnOMIP/CPE were prepared by mixing the appropriate amount of the synthesized modifier, graphite powder and paraffin oil (20:55:25 w/w %).

Preparation of the Real Samples

To evaluate the efficiency of the method, BPA was determined in various real samples to include tap water, food storage container, and cured vinyl ester resin. The tap water was collected and directly analyzed after pH adjustment.

For analysis, the polymer samples, food storage container was purchased from the local market, and vinyl ester resin was prepared from Farapol Jam chemical industries Co. with a code of V 301. The V 301 resin was cured by addition of 1% Cobalt Octoate (1% in styrene), 0.5% Dimethyl aniline (10% in styrene) and 1% AKPEROX A60 as catalyst. After 24 h, in order to reach a maximum number of cross-linked polymerization, the cured V 301 resin was placed in the oven at 80 °C for 2 h and 1 h at 120 °C. The polymer samples were cut into pieces about 0.2-0.5 g and put into the flask for 40 min in 50 ml DDW, which was then kept at 70 °C. In the next step, the obtained mixture was cooled to ambient temperature, filtered, and collected in a beaker. The extraction of BPA on the selected sample piece was repeated three times. For analysis, 10.0 ml of the whole collected sample was poured into a 25 ml volumetric flask contained B-R pH = 6.5.

RESULTS AND DISCUSSION

Investigation of the Synthesized Materials

The structural specifications of the synthesized materials were checked *via* several methods including FTIR spectroscopy, TGA, XRD and SEM.

The FTIR spectra of GO, rGO, Fe_3O_4 NPs, ZnO NPs, rGO-Fe_3O_4 and rGO-Fe_3O_4-ZnO nanocomposites are presented in Fig. 1a. The FTIR spectrum of GO shows specific peaks about 3400, 2860, 1740, 1650, 1400 and 1250 cm^{-1}, which corresponds to O-H stretching, C-H stretching, C=O stretching, C-O-H vibration, C-O stretching related to the phenolic group, and C=C stretching related to aromatic rings, respectively. As can be seen, the absorption band of oxide groups in spectra of rGO has decreased

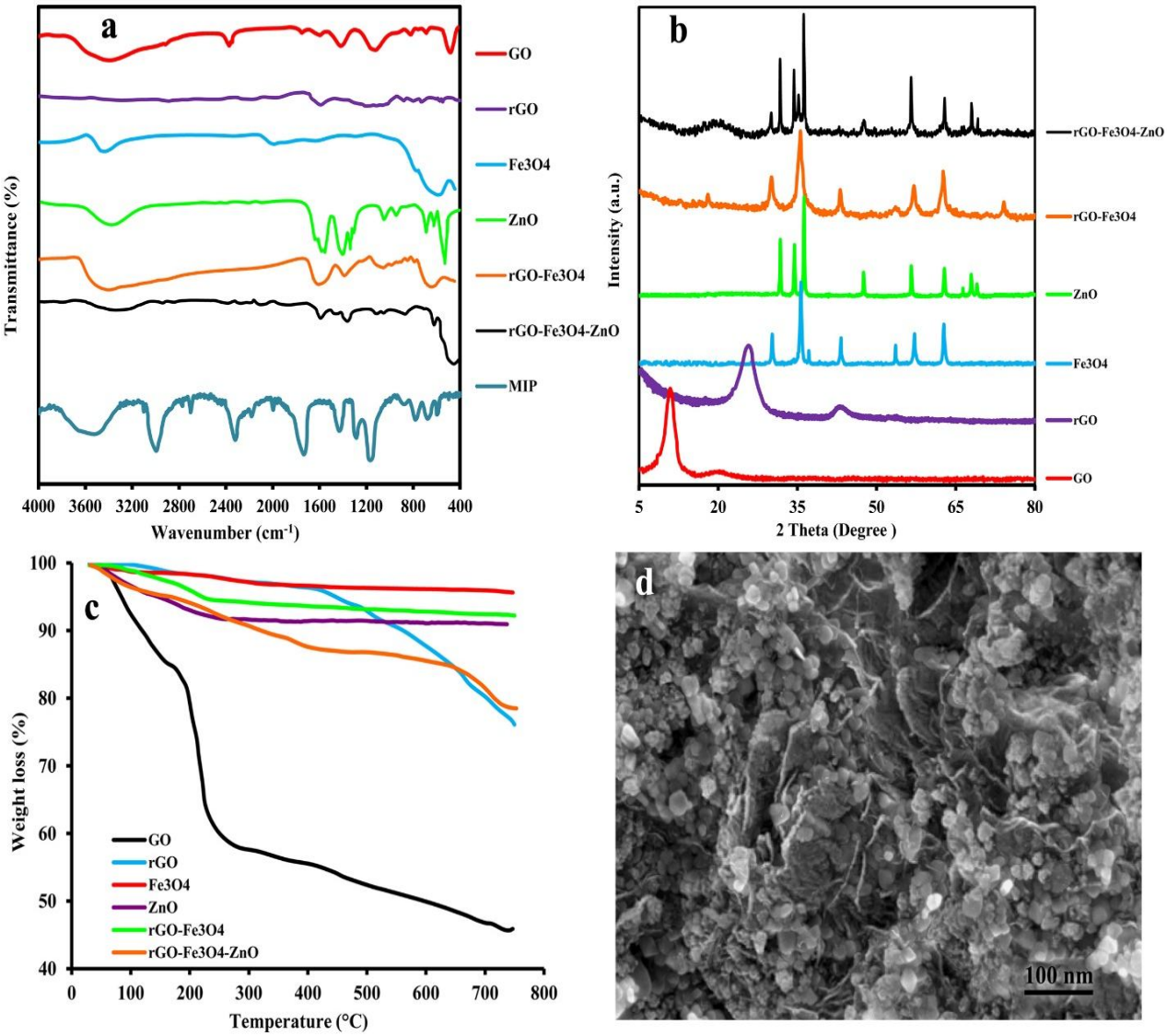

Fig. 1. (a) The FTIR spectra (b) the XRD patterns; (c) TGA analysis of the synthesized GO, rGO, Fe_3O_4 NPs, ZnO NPs, rGO-Fe_3O_4 and rGO-Fe_3O_4-ZnO nanocomposites; (d) SEM image of rGO-Fe_3O_4-ZnO nanocomposites.

significantly after applying the chemical reduction process [34]. For Fe_3O_4 NPs, an intense peak of about 560-570 cm^{-1} can be related to the stretching vibration of the Fe-O bond, and the peak of about 3500 could be originated by the presence of the OH group in absorbed water [35]. In the case of ZnO, the observed peak at 530 cm^{-1} is related to Zn-O stretching vibrations. The peaks at 3350 cm^{-1} can correspond to the stretching vibration of the OH group (adsorbed H_2O in the samples) [36]. In the FTIR spectrum of rGO-Fe_3O_4, the broad absorption peak at 3400 cm^{-1} can be due to stretching vibrations of OH groups on the rGO and adsorbed H_2O in the surface of synthesized rGO-Fe_3O_4. Also, in the absorption peaks at 1050 cm^{-1} (C-O stretching vibration), 1370 cm^{-1} (C-OH groups stretching), and

1650 cm^{-1} (C=O stretching) can be observed. In addition, the peak at 610 cm^{-1} can be related to the stretching vibration of Fe-O. The shift of the peak of Fe-O bond in the rGO-Fe_3O_4 nanocomposite can be caused by that chemically bonded of Fe_3O_4 NPs with the surface of rGO (interaction occur between O and Fe). The FTIR spectrum of rGO-Fe_3O_4-ZnO nanocomposite shows several peaks which are related to Zn-O (500 cm^{-1}), Fe-O (565 cm^{-1}), C-O (1055 cm^{-1}), C-OH (1360 cm^{-1}), -OH (3350 cm^{-1}) and C=O (1600 cm^{-1}), so it can be concluded that the rGO-Fe_3O_4-ZnO nanocomposite was synthesized successfully.

For the investigation of the structure of the synthesized materials, the XRD analysis was applied, and obtained results are shown in Fig. 1b. The XRD patterns of GO and rGO illustrate typical characteristic peaks at 2θ = 10° and 25°, respectively, which they are fit well with previous reports which indicated the successful synthesis of GO and rGO. So, the results confirm that GO is converted completely to rGO by sodium borohydride. All obtained peaks of the XRD pattern for Fe_3O_4 NPs were matched truly to the pattern of reported Fe_3O_4 NPs (JCPDS No. 01-176-1849) which informing the high purity of synthesized nanoparticles [37]. The XRD pattern of ZnO NPs represents seven peaks at 31.78°, 34.44°, 36.25°, 47.54°, 56.58°, 62.85° and 67.95° which confirm that the ZnO NPs was synthesized without any impurities [38]. For rGO-Fe_3O_4 observed peaks were similar to Fe_3O_4 NPs. In the XRD pattern of the rGO-Fe_3O_4-ZnO nanocomposite, the peaks related to rGO (about 23°), Fe_3O_4 NPs (30°, 35.12°, 43.02°, 57.09° and 62.63°) and ZnO NPs (31.67°, 47.56° and 67.99°) were observed which corroborate the well synthesize of target nanocomposite.

The obtained results of TGA analysis for investigation of the thermal stability of GO, rGO, Fe_3O_4, ZnO, rGO-Fe_3O_4 and rGO-Fe_3O_4-ZnO nanocomposites are depicted in Fig. 1c. As can be seen, the GO sheet is an unstable thermally material which weight loss of it occurs in three stages. The release of absorbed water from the surface of GO occurs below 100 °C by 10% weight loss. The removal of trapped water molecules and epoxy oxygen functional groups happened between 100 and 250 °C (about 30% weight loss). Also, the removal of phenolic groups and decomposition of carbon atoms with sp^3 hybridization occurred at 500 °C. The results demonstrate that rGO is more thermally stable than GO, and almost no weight loss was observed below 500 °C (less than 5%). The obtained result indicates that the reduction of GO was done effectively, and oxygen functional groups removed successfully. Fe_3O_4 NPs show a total weight loss of about 4.4, indicating the higher thermal stability of this nanoparticle. The TGA for ZnO NPs shows a weight loss of about 5% at below 100 °C, which can be due to the release of absorbed water and after that no weight loss was observed which demonstrates the stability of the nanoparticle [39,40]. The result of TGA analysis proves the high stability of rGO-Fe_3O_4 nanocomposite (weight loss about 7% at 750 °C). For rGO-Fe_3O_4-ZnO nanocomposite a weight loss of 4.5% at 120 °C and 8.3% at 400 °C are related to the evaporation of the adsorbed water and loss of CO, CO_2 arising from the pyrolysis of oxygen groups. A considerable mass loss at a higher temperature could be owing to the bulk pyrolysis of the carbon skeleton [41].

In order to the investigation of size, morphology and uniformity of synthesized nanocomposites, the SEM analysis was carried out. The SEM image in Fig. 1d shows the morphology of the prepared rGO-Fe_3O_4-ZnO nanocomposite with an average size of approximately 30 nm. It can be seen that the provided results by FTIR, XRD and SEM analysis confirmed the successful formation of the rGO-Fe_3O_4-ZnO nanocomposite.

Investigation Electrochemical Reactivity of the Constructed Electrodes

The electrochemical activity, charge transferability and the surface properties of the modified and bare sensors were investigated in the presence of 5.0 mM $[Fe(CN)_6]^{3-/4-}$ and 1.0 M KCl by the cyclic voltammetric technique (CV) and Electrochemical impedance spectroscopy (EIS).

The CVs of CPE, MIP/CPE, NIP/CPE, GOMIP/CPE, rGOMIP/CPE, Fe_3O_4MIP/CPE, ZnOMIP/CPE, rGO-Fe_3O_4MIP/CPE and rGO-Fe_3O_4-ZnOMIP/CPE are depicted in Fig. 2a. As can be seen, the peak current (Ip) and the peak potential separation (ΔEp) were dependent on the sensing layer of electrodes.

The $[Fe(CN)_6]^{3-/4-}$ represents a pair of weak redox peaks (Ip = 68.05 μA) with ΔE_p = 267 mV by using the unmodified CPE. The Ip and ΔEp have increased while the

MIP/CPE was used as working electrode (Ip = 85.32 μA, ΔE_p = 279). On the other hand, the Ip and ΔEp have decreased and increased respectively, while NIP/CPE was used for recording the redox reaction of the probe (I_p = 52.33 μA, ΔE_p = 303). It demonstrates that there were more redox sites and channels on the surface of MIP/CPE after elution in comparison to NIP/CPE.

On the surface of GOMIP/CPE, ZnOMIP/CPE, rGOMIP/CPE, Fe_3O_4MIP/CPE, rGO-Fe_3O_4MIP/CPE and rGO-Fe_3O_4-ZnOMIP/CPE, two well-defined peaks appeared by I_p 82.92, 110.87, 139.41, 142.73, 187.04 and 220.76 μA respectively. Also, the ΔE_p for mentioned electrodes have decreased gradually. This phenomenon was owning to increase the conductivity and surface area of using nanoparticles and nanocomposites. The highest I_p (220.76 μA) and the lowest ΔE_p (151 mV) are obtained when the CPE was modified by rGO-Fe_3O_4-ZnOMIP which can be related to the synergistic effect between Fe_3O_4 and ZnO nanoparticles and rGO, which then lead to boost in catalytic ability, electron transfer rate, number of reaction site and conductivity.

Electrochemical impedance spectroscopy (EIS) is an electrochemical technique to measure the impedance of system independence on the AC potentials frequency. EIS is one of the most complex techniques in electrochemical research. This study was employed to investigate the characteristics of the probe layers on the electrochemical sensors. In EIS, the semicircular part at higher frequencies and linear part at lower frequencies correspond to the electron transfer resistance (R_{ct}) and limited diffusion process, respectively. The diameter of the semicircle equals R_{ct} represents the difficulty of electron transfer of a ferrocyanide-redox probe between the solution and the electrode, supplying information of the electrochemical interphase.

In order to check the surface properties and charge transferability of the prepared electrodes, the EIS analysis was applied, and the results are shown in Fig. 2b. The R_{ct} values were obtained 4179, 3790, 2958, 2626, 2283, 1810, 1337, 607 and 468 Ω for the NIP/CPE, MIP/CPE, CPE, GOMIP/CPE, ZnOMIP/CPE, rGOMIP/CPE, Fe_3O_4MIP/CPE, rGO-Fe_3O_4MIP/CPE and rGO-Fe_3O_4-ZnOMIP/CPE, respectively. As can be seen, the impedance value of NIP/CPE is more than MIP/CPE; it owns to the creation of many cavities into the surface of the MIP film after removal of BPA, which is useful for $[Fe(CN)_6]^{3-/4-}$ to get into the MIP on the surface of the MIP/CPE. By modification of MIP with different nanoparticles and nanocomposites, based on the conductivity of them and development of reaction site on the surface of the electrode, the impedance of CPE, GOMIP/CPE, ZnOMIP/CPE, rGOMIP/CPE, Fe_3O_4MIP/CPE, rGO-Fe_3O_4MIP/CPE and rGO-Fe_3O_4-ZnOMIP/CPE have reduced gradually.

The acquired data confirm that rGO-Fe_3O_4-ZnOMIP/CPE which has the maximum Ip, lowest ΔEp and Rct is the best candidate for use in electrochemical application among the other electrodes.

Voltammetric Studies of BPA on the Different Electrodes

DPV technique investigated the voltammetric behavior of 5 μM BPA in B-R buffer solution pH = 6.5 at the surface of unmodified CPE, and MIP/CPE, NIP/CPE, GOMIP/CPE, rGOMIP/CPE, Fe_3O4MIP/CPE, ZnOMIP/CPE, rGO-Fe_3O_4MIP/CPE and rGO-Fe_3O_4-ZnOMIP/CPE and the result is depicted in Fig. 3a.

It can be seen; the unmodified CPE shows broad and ill-defined oxidation peaks (I_p = 1.03 μA) at 650 mV. By using NIP/CPE and MIP/CPE as working electrode, an oxidation peak by more oxidation current were observed, while the obtained current of MIP/CPE is more than NIP/CPE. This phenomenon occurs due to the presence of porous structure of MIP at the surface of CPE.

One sharp oxidation peak appeared with Ip about 8.6 μA for BPA at the surface of GOMIP/CPE and ZnOMIP/CPE. The increase in currents in comparison to MIP/CPE is related to an increase in the surface and electrochemical site of GOMIP/CPE and ZnOMIP/CPE because of the use of GO or ZnO NPs. Also, by using the rGO for modification of MIP/CPE, the conductivity of rGOMIP/CPE has enhancement significantly, and a peak with Ip=10.78 μA appeared. The Fe_3O_4MIP/CPE, and rGO-Fe_3O_4MIP/CPE show a peak with Ip = 11.76 and 13.07 μA respectively. The modified CPE with rGO-Fe_3O_4-ZnOMIP nanocomposite represents an excellent improvement in the Ip, and a well-defined peak for BPA by Ip = 16 μA at 648 mV appeared. Also, in the absence of BPA, the rGO-Fe_3O_4-ZnOMIP/CPE did not show any oxidation peaks in the potential region

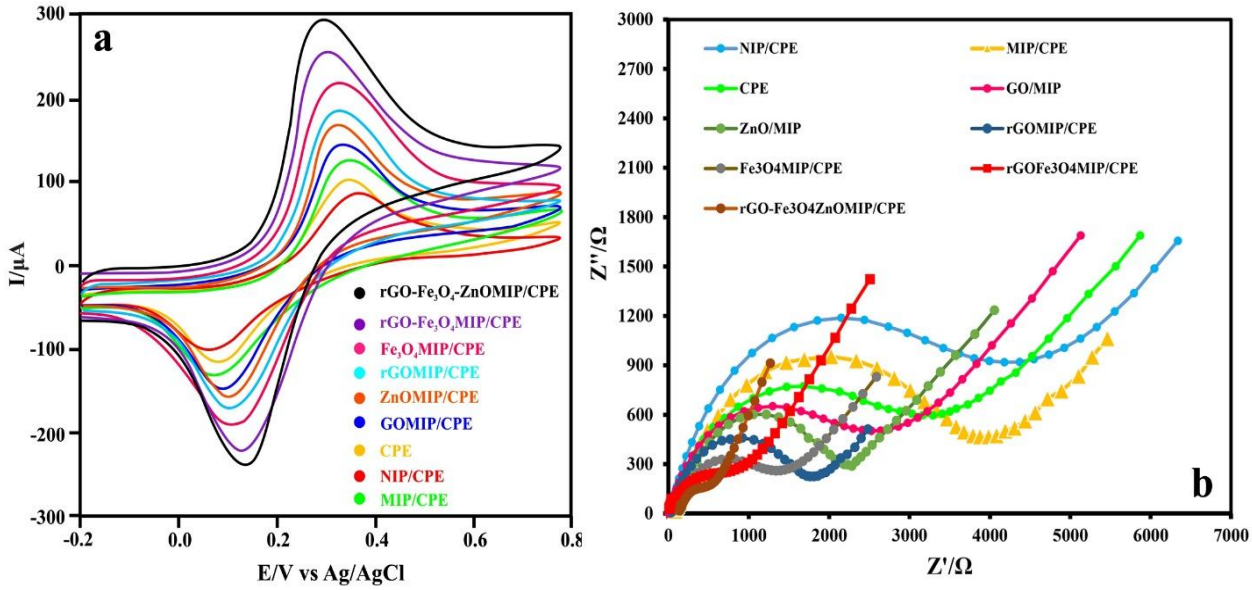

Fig. 2. (a) CVs and (b) Nyquist plots of the bare CPE, MIP/CPE, NIP/CPE, GOMIP/CPE, rGOMIP/CPE, Fe_3O_4MIP/CPE, ZnOMIP/CPE, rGO-Fe_3O_4MIP/CPE and rGO-Fe_3O_4-ZnOMIP/CPE in 5.0 mM $[Fe(CN)_6]^{3-/4-}$ and 1.0 M KCl.

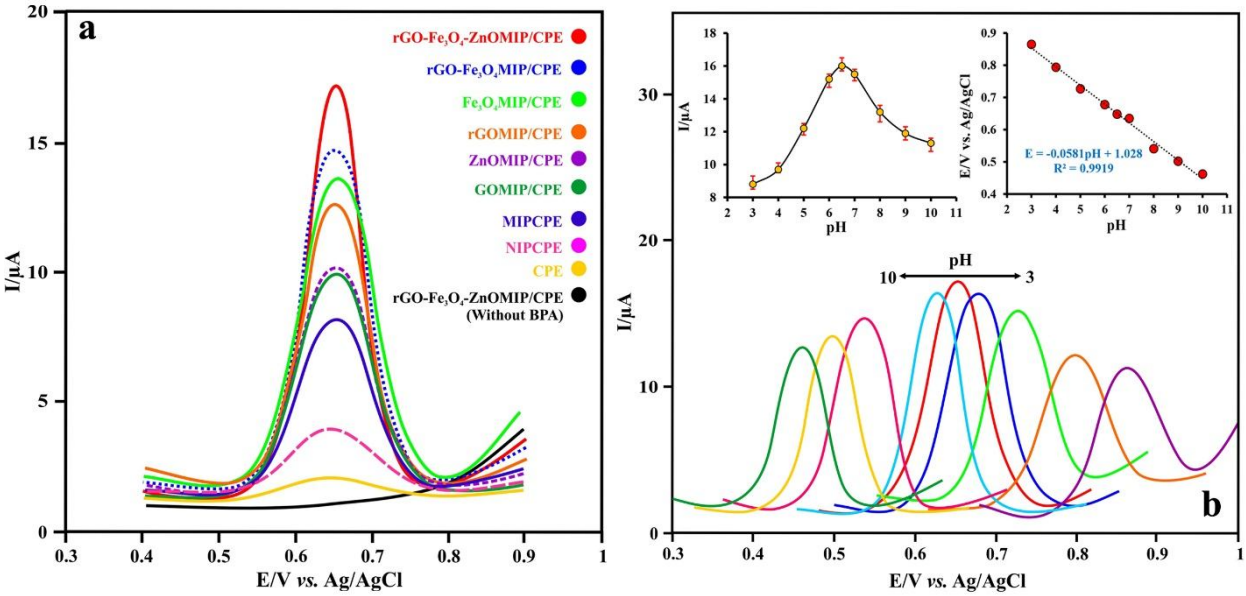

Fig. 3. (a) DPVs of 5 µM BPA at the surface of CPE, and MIP/CPE, NIP/CPE, GOMIP/CPE, rGOMIP/CPE, Fe_3O_4MIP/CPE, ZnOMIP/CPE, rGO-Fe_3O_4MIP/CPE and rGO-Fe_3O_4-ZnOMIP/CPE and in the absence of the analyte (b) The DPV of 5 µM BPA at rGO-Fe_3O_4-ZnOMIP/CPE at different pH between 3 and 10; (Inset: The influence of pH on potential of peak and current of the analyte).

0.4-0.9 V. Based on the data rGO-Fe_3O_4-ZnOMIP/CPE is the best choice for the determination of the BPA with a low detection limit (DL) and high sensitivity.

Fe_3O_4-ZnOMIP/CPE

Since the electrochemical oxidation of BPA involves both hydrogen ions and electrons [16], so the variation in pH can change the potential and current of 5 µM BPA oxidation peak at the surface of rGO-Fe_3O_4-ZnOMIP/CPE. Therefore, the electrochemical behavior of BPA at the rGO-Fe_3O_4-ZnOMIP/CPE was studied at different pH values between 3 and 10 using DPV (Fig. 3b).

The results demonstrate that the oxidation peak potential of BPA has shifted to more negative potential values when the pH has changed from 3 to 10. The graph of the peaks potential versus pHs is shown in Fig. 3b with the linear regression equation of Epa = -0.0581pH + 1.028 (R^2 = 0.9919). The slope of the equation is about the Nernstian slope value (0.059 V/pH at 25 °C) which demonstrated that the number of H^+ and electrons is equal. Following prior reports, the number of H^+ and electrons that participated in the oxidation of BPA are two electrons and two protons.

The oxidation current of BPA at rGO-Fe_3O_4-ZnOMIP/CPE was checked at different pH values. The data show that Ip has increased with growing the pH values, and the maximum value was obtained at pH = 6.5 (Fig. 3b). By increasing the pH from 6.5 to 10, the peak currents have declined. So, to arrive at the best sensitivity and selectivity for the determination of BPA by rGO-Fe_3O_4-ZnOMIP/CPE, pH = 6.5 was selected as the optimum value.

The Impact of Scan Rate on the Electro-Oxidation of BPA at rGO-Fe_3O_4-ZnOMIP/CPE

CV was applied to study the kinetics of the proposed electrode reaction for 10 µM BPA at rGO-Fe_3O_4-ZnOMIP/CPE at scan rates of 25, 50, 100, 150, 200, 250 and 300 mV s^{-1} (Fig. 4a). The obtained CVs for BPA represent that the oxidation peak currents have increased by growing the scan rate by the equation of I = 0.2462v - 2.5744 (R^2 = 0.9954), so it can be said that the oxidation of BPA at rGO-Fe_3O_4-ZnOMIP/CPE is an adsorption controlled process.

In addition, the oxidation peak potentials of BPA have moved to more positive potentials by increasing the scan rate and the relationship between the potential of peak and the logarithm of scan rate was Ep = 0.0278 Lnv + 0.5199 (R^2 = 0.9953).

Laviron shows that in an irreversible electrochemical reaction with an adsorption-controlled process, the relationship between the potential of peak and the logarithm of scan rate is expressed by Ep = E^0 + $(RT/\alpha nF)$ ln$(RTK0/\alpha nF)$ + $(RT/\alpha nF)$ ln$v$.

As observed, the slop was obtained 0.0278, and generally is considered to be 0.5 for irreversible electrochemical reaction, T = 298 K, R = 8.314 J $Kmol^{-1}$ and F = 96485 C mol^{-1}, so the electron transfer number (n) was calculated 1.85 which is near to the theoretical amount of 2 for electro-oxidation of BPA. Based on pH investigation and calculated n, the proposed mechanism is presented in Scheme 1.

Effect of Accumulation Time

Since the electro-oxidation of BPA at rGO-Fe_3O_4-ZnOMIP/CPE was an adsorption controlled process, the number of BPA molecules on the electrode surface has increased significantly by applying the accumulation time and influences the adsorption yield so the oxidation current of the target analyte has improved. This accumulation process between BPA and rGO-Fe_3O_4-ZnOMIP/CPE was carried out using a mechanical stirrer.

The impact of accumulation time on the peak current of BPA at rGO-Fe_3O_4-ZnOMIP/CPE is shown in Fig. 4b, and it can be seen that the oxidation peak currents have grown gradually with increasing the accumulation time and after 200 s it reached a plateau and the currents remained nearly constant. So, in order to earn the best DL and sensitivity, the accumulation time of 200 s was chosen as the optimal deposition time of BPA on the surface of rGO-Fe_3O_4-ZnOMIP/CPE.

Voltammetric Calibration Plot, Repeatability and Reproducibility of BPA Detection at rGO-Fe_3O_4-ZnOMIP/CPE

The effect of BPA concentration on oxidation peak currents at rGO-Fe_3O_4-ZnOMIP/CPE was investigated using DPV in 0.1 M B-R buffer solution with pH = 6.5 and the voltammograms and calibration curve are depicted in

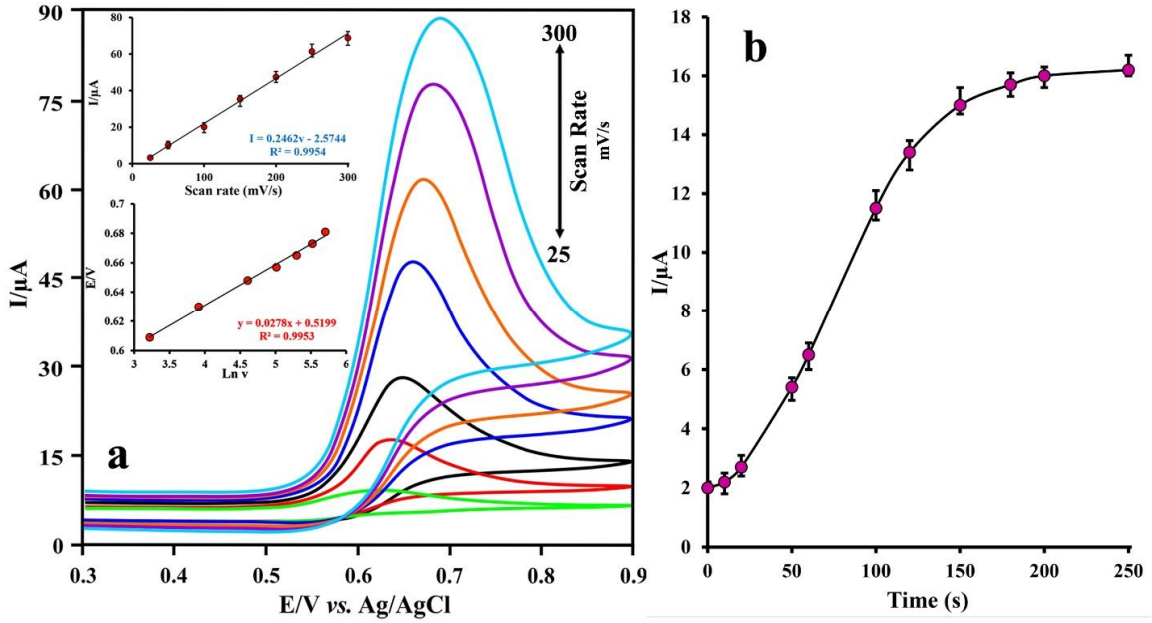

Fig. 4. (a) CVs at rGO-Fe_3O_4-ZnOMIP/CPE in B-R buffer solution with pH 6.5 containing 10 µM BPA with scan rates ranging from 25 to 300 mV s^{-1}; (Insert: the linear relationship between Ip *vs*. scan rate and Ep *vs*. Ln scan rate); (b) The effect of accommodation time on peak current.

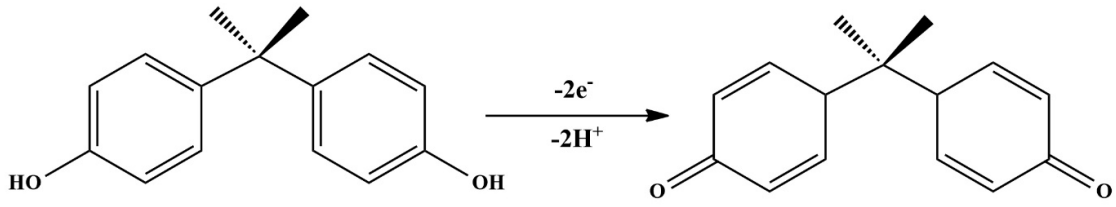

Scheme 1. Proposed electrochemical oxidation mechanism for BPA

Fig 5. Determination of BPA was examined at the optimal condition while the concentration of it was changed in the range of 0.008-15 and 15-95 µM with the regression equation of Ip = 3.1097C + 0.7873 (R^2 = 0.998) and Ip = 1.5753C + 23.608 (R^2 = 0.9982), respectively. The obtained DL was 0.004 µM and computed as three times the standard deviation of the blank over sensitivity (3Sb/m).

The repeatability and reproducibility of the suggested electrode were checked out with five measurements for 10 µM BPA at rGO-Fe_3O_4-ZnOMIP/CPE in one day and five days respectively and the respective relative standard deviations (RSD) were reported. The calculated RSD% for repeatability and reproducibility tests were 3.1%, and 3.5%, respectively, which illustrate the acceptable repeatability and reproducibility of the sensor.

Interference and Stability Studies

The interference possibility of various compounds in the determination of 1 µM BPA at rGO-Fe_3O_4-ZnOMIP/CPE was checked by the addition of compounds to 0.1 M B-R

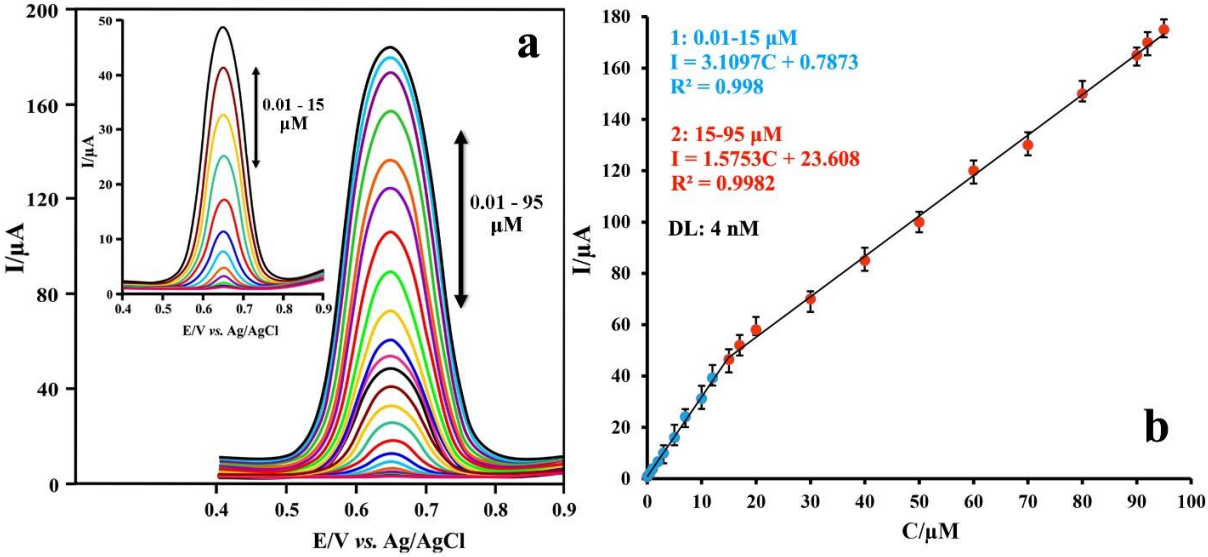

Fig. 5. (a) DPVs of different concentration of BPA at rGO-Fe_3O_4-ZnOMIP/CPE in B-R buffer solution pH = 6.5; (b) Calibration plots.

Table 1. Determination of the BPA in Different Real Samples

Sample	Added (µM)	Found (µM)	Recovery (%)
Tap water	0.0	Not detected	-
	5.0	5.18	103.6
	10.0	10.34	103.4
Food storage container	0.0	4.52	-
	5.0	9.41	97.8
	10.0	14.73	102.1
Cured vinyl ester resin (Farapol V 301)	0.0	0.18	-
	5.0	5.12	98.8
	10.0	10.29	101.1

buffer solution with pH = 6.5. The anodic peak current of BPA was measured in the absence and presence of different concentrations of interference species, and then the change in the oxidation peak currents was checked out. The data show that K^+, Na^+, Cl^-, Mg^{2+}, Ca^{2+}, Al^{3+}, NO_3^-, SO_4^{2-}, SO_3^{2-}, ClO^{4-} and CO_3^{2-} had no disturbance on the detection of

Table 2. Comparison between Presented Method and Recent Electrochemical Methods for Determination of BPA

Electrode	Method	LR (μM)	LD (μM)	Refs.
MIPs/AuNPs/GCE	LSV	0.015-55	0.0011	[42]
GO/APTES-MIP/GCE	DPV	0.006-20	0.003	[43]
Graphene/Au/GCE	LSV	0.08-250	0.035	[44]
MWCNT/MIP/CPE	DPV	0.08-100	0.022	[45]
MIP/chitosan/graphene/ABPE	DPV	0.008-1	0.006	[46]
PEDOT/GCE	CV	90-410	55	[47]
AuNPs/CBNPs/SPCE	DPV	0.07-10	0.0088	[48]
Na-doped WO3/CPE	DPV	0.081-22.5	0.028	[49]
CTS-GR/CILE	DPV	0.1-800	0.026	[50]
Au-Cu@BSA/GCE	SWASV	0.01-70	0.004	[16]
rGO-Fe_3O_4-ZnOMIP/CPE	DPV	0.01-15 15-95	0.004	Presented work

BPA.

The effect of other species includes Hydroquinone, Tert-butyl hydroquinone, Catechol and Bisphenol S were investigated. The data show that Hydroquinone, Tert-butyl hydroquinone, Catechol and Bisphenol S had no disturbance on the detection of BPA and the change in peak current was below 5% when the concentration of substances were 160, 210, 115 and 25 times more than BPA. The obtained data show high selectivity of the presented electrode.

The stability on a long time of rGO-Fe_3O_4-ZnOMIP/CPE was investigated by measurement of the anodic peak currents of 5 μM BPA in different days by a constructed electrode, and the electrode was immersed in the buffer solution and maintained at ambient temperature when it was not used. After 25 days, the oxidation current of BPA was approximately stable and has changed below 5%, which indicates the high stability of rGO-Fe_3O_4-ZnOMIP/CPE.

Real Sample and Spiked Samples Analysis

The proposed electrochemical sensor was validated for the determination of BPA in the different real samples and spiked samples including tap water, food storage container and cured vinyl ester resin by DPV technique. The obtained results of the samples were presented in Table 1. The recovery percentages of spiked samples were between 97.8 and 103.8%, which displays the potency of the proposed method to the measurement of BPA in different matrices.

CONCLUSIONS

In the presented research, the rGO, Fe_3O_4 and ZnO NPs were used for the synthesis of rGO-Fe_3O_4-ZnO nanocomposite and applied for modification of MIP sensing layer in order to selective determination of BPA. The rGO-Fe_3O_4-ZnOMIP/CPE shows high repeatability, reproducibility, stability, excellent conductivity and high

selectivity. DPV was carried out for the determination of BPA with a wide linear range (0.008-15 and 15-95 μM) and a low detection limit (0.004 μM). Table 2 shows the linear range and DL based on μM for the recent electrochemical methods for the determination of BPA. It can be seen that the presented method has good analytical performance in comparison to most of the previous methods. The rGO-Fe_3O_4-ZnOMIP/CPE was successfully applied for the measurements of BPA in tap water, food storage container and cured vinyl ester resin samples with admissible recovery percentages between 97.8 and 103.8%. Finally, it can be said that a new modified electrode with the simplicity of constructing and several mentioned advantages could be introduced for analytical applications in quality control of companies.

REFERENCES

[1] T. Kemper, S. Sommer, Environ. Sci. Technol. 36 (2002) 2742.

[2] X.-H. Wu, D.-H. Sun, Z.-X. Zhuang, X.-R. Wang, H.-F. Gong, J.-X. Hong, F.S.C. Lee, Anal. Chim. Acta 453 (2002) 311.

[3] H.-W. Sun, F.-X. Qiao, R. Suo, L.-X. Li, S.-X. Liang, Anal. Chim. Acta 505 (2004) 255.

[4] P. Bermejo-Barrera, Ó. Muñiz-Naveiro, A. Moreda-Piñeiro, A. Bermejo-Barrera, Anal. Chim. Acta 439 (2001) 211.

[5] F.R. Moreira, M.G. Mello, R.C. Campos, Spectrochim. Acta, Part B 62 (2007) 1273.

[6] S. Li, S. Cai, W. Hu, H. Chen, H. Liu, Spectrochim. Acta, Part B 64 (2009) 666.

[7] I. Boevski, N. Daskalova, I. Havezov, Spectrochim. Acta, Part B 55 (2000) 1643.

[8] E. Webb, D. Amarasiriwardena, S. Tauch, E.F. Green, J. Jones, A.H. Goodman, Microchem. J. 81 (2005) 201.

[9] H. Karami, M.F. Mousavi, Y. Yamini, M. Shamsipur, Anal. Chim. Acta 509 (2004) 89.

[10] G. Alloncle, N. Gilon, C.-P. Lienemann, S. Morin, C. R. Chim. 12 (2009) 637.

[11] S. Ashoka, B.M. Peake, G. Bremner, K.J. Hageman, M.R. Reid, Anal. Chim. Acta 653 (2009) 191.

[12] J. Barciela, M. Vilar, S. García-Martín, R.M. Peña, C. Herrero, Anal. Chim. Acta 628 (2008) 33.

[13] Y. Ni, Anal. Chim. Acta 284 (1993) 199.

[14] V. Kaur, J.S. Aulakh, A.K. Malik, Anal. Chim. Acta 603 (2007) 44.

[15] S. Oszwałdowski, R. Lipka, M. Jarosz, Anal. Chim. Acta 361 (1998) 177.

[16] U.S. Hong, H.K. Kwon, H. Nam, G.S. Cha, K.-H. Kwon, K.-J. Paeng, Anal. Chim. Acta 315 (1995) 303.

[17] S.B. Khoo, S.X. Guo, Electroanalysis 14 (2002) 813.

[18] F. Qneirolo, P. Valenta, Anal. Chem. 328 (1987) 93.

[19] Ø. Mikkelsen, K.H. Schrøder, Electroanalysis 15 (2003) 679.

[20] J. Wang, B. Anal. Chem. 65 (1993) 1529.

[21] X.-H. Zhang, S.-F. Wang, Sens. Actuators, B 104 (2005) 29.

[22] M. Brand, I. Eshkenazi, E. Kirowa-Eisner, Anal. Chem. 69 (1997) 4660.

[23] B. Krasnodębska-Ostręga, J. Piekarska, Electroanalysis 17 (2005) 815.

[24] J. Di, F. Zhang, Talanta 60 (2003) 31.

[25] P. Calvo-Marzal, K.Y. Chumbimuni-Torres, N.F. Höehr, G. de Oliveira Neto, L.T. Kubota, Sens. Actuators, B 100 (2004) 333.

[26] J.-B. He, C.-L. Chen, J.-H. Liu, Sens. Actuators, B 99 (2004) 1.

[27] M. Mazloum-Ardakani, A. Khoshroo, L. Hosseinzadeh, Sens. Actuators, B 204 (2014) 282.

[28] N. Maleki, A. Safavi, F. Tajabadi, Anal. Chem. 78 (2006) 3820.

[29] A.A. Ensafi, N. Ahmadi, B. Rezaei, M.M. Abarghoui, Talanta 134 (2015) 745.

[30] R.A. Dar, P.K. Brahman, S. Tiwari, K.S. Pitre, Colloids Surf., B 91 (2012) 10.

[31] A. Afkhami, H. Khoshsafar, H. Bagheri, T. Madrakian, Sens. Actuators, B 203 (2014) 909.

[32] G. Aragay, A. Merkoçi, Electrochim. Acta 84 (2012) 49.

[33] H. Bagheri, A. Afkhami, A. Shirzadmehr, H. Khoshsafar, H. Khoshsafar, H. Ghaedi, Int. J. Environ. Anal. Chem. 93 (2012) 578.

[34] F. Campbell, R. Compton, Anal. Bioanal. Chem. 396 (2010) 241.

[35] H. Bagheri, A. Afkhami, H. Khoshsafar, M. Rezaei,

A. Shirzadmehr, Sens. Actuators, B 186 (2013) 451.

[36] A. Afkhami, T. Madrakian, S.J. Sabounchei, M. Rezaei, S. Samiee, M. Pourshahbaz, Sens. Actuators, B 161 (2012) 542.

[37] H. Deng, X. Li, Q. Peng, X. Wang, J. Chen, Y. Li, Angew. Chem., Int. Ed. 44 (2005) 2782.

[38] S.J. Sabounchei, S. Samiee, D. Nematollahi, A. Naghipour, D. Morales-Morales, Inorg. Chim. Acta 363 (2010) 3973.

[39] T. Madrakian, A. Afkhami, M. Ahmadi, Chemosphere 90 (2013) 542.

[40] L. Luo, X. Wang, Y. Ding, Q. Li, J. Jia, D. Deng, Appl. Clay Sci. 50 (2010) 154.

[41] R. Pauliukaitė, C.M.A. Brett, Electroanalysis 17 (2005) 1354.